JMM

Horseshoe dynamics in Duffing oscillator with fractional damping and multi-frequency excitation

S. Valli Priyatharsini[†], M.V. Sethu Meenakshi[‡], V. Chinnathambi[†*] and S. Rajasekar[§§]

[†]*Department of Physics, Sadakathullah Appa College, Tirunelveli-627 011, Tamil Nadu, India (Affiliated to Manonmaniam Sundaranar University, Tirunelveli-627012, Tamil Nadu, India)*

[‡]*Department of Mathematics, St. Xavier's College, Tirunelveli -627 002, Tamil Nadu, India*
[§§]*School of Physics, Bharathidasan University, Tiruchirapalli-620 024, Tamil Nadu, India*
Emails: svallipriyatharsini@gmail.com, sethumeenakshi91@gmail.com, drchinnathambi@sadakath.ac.in, rajasekar@physics.bdu.ac.in

Abstract. The occurrence of horseshoe chaos in Duffing oscillator with fractional damping and multi-frequency excitation is analyzed by using analytical and numerical techniques. Applying Melnikov method, analytical threshold condition for the onset of horseshoe chaos is obtained. The effect of damping exponent and the number of periodic forces on the dynamics of the Duffing oscillator is also analyzed. Due to fractional damping and multi-frequency excitation, suppression of chaos and various nonlinear phenomena are predicted. Analytical predictions are demonstrated through numerical simulations.

Keywords: Duffing oscillator, Fractional damping, Horseshoe chaos, Melnikov method, Multi-frequency excitation.
AMS Subject Classification: 37D45, 37J20, 37C29.

http://jmm.guilan.ac.ir

1   Introduction and motivation

Horseshoe chaos is a very interesting nonlinear phenomena, and it has been detected in a large number of nonlinear systems of various physical nature [3,6,16,17,20,27]. Horseshoe is the occurrence of transverse intersection of stable and unstable manifolds of a saddle fixed point in the Poincaré map, and is a global phenomena. Its appearance can be predicted analytically by employing the Melnikov technique. This technique essentially gives a criterion for a transverse intersection of the stable and unstable manifolds of homoclinic or heteroclinic orbits which imply horseshoe chaos. The essence of this method is to calculate the so called Melnikov integral, which can be used to identify the regions in the parameter space where horseshoe chaos occurs. Recently, this method has been applied to certain nonlinear systems to predict the occurrence of horseshoe chaos [17–21,25].

In the recent years there has been a great deal of interest in the study of the effect of multi-frequency excitation in certain linearly damped nonlinear systems [4, 5, 7–10, 15]. In the present paper we study the occurrence of horseshoe chaos in Duffing oscillator with fractional damping and multi-frequency excitation both analytical and numerical techniques.

The Duffing oscillator driven by multi-frequency excitation with fractional damping is given as

$$\ddot{x} + \alpha \, \dot{x} \, |\dot{x}|^{P-1} - \omega_0^2 x + \beta x^3 = \sum_{i=1}^{k} f_i \sin \omega_i t, \tag{1}$$

where x stands for the displacement from the equilibrium point, $\alpha > 0, \beta > 0$ and $\omega_0^2 > 0$ are the damping coefficient, coefficient of stiffness and natural frequency of the system respectively. P is the damping exponent, f and ω are the amplitude and frequency of the external force. The motivation for our interest in this system is that it is one of the simplest nonlinear dissipative models with a wide range of complex behaivour. It is used for the description of many real processes, such as mechanical and radio physical oscillators (see [6,14] and references therein), plasma dynamics [12] and others. The properties of the Duffing system have been widely analyzed in particular using the Melnikov method [6,11,13].

In Eq. (1) the fractional damping term is taken to be proportional to the power of velocity $\dot{x}$ in the form $|\dot{x}|^{P-1}$. A similar nonlinear term was previously used by many researchers [1,2,22–24,26]. The objective here is to explore the occurrence of horseshoe chaos in the system (1) using analytical and numerical techniques. In the present paper, we use Melnikov method to study the influence of multi-frequency force and fractional damping term.

The paper is organized as follows. In Section 2, we obtain the Melnikov function for the system (1) by treating the damping term and external excitation with weak perturbation. In Section 3, we analyze the occurrence of horseshoe chaos and asymptotic chaos using Melnikov method. Numerical results and its discussion are presented in Section 4. We show some examples of various nonlinear phenomena for some specific set of values of the parameters. Finally, Section 5 contains the summary of the present work.

2 Melnikov function

In the section, we provide the details of the Melnikov analysis for the Duffing oscillator with fractional damping driven by multi-frequency force. We consider the perturbed Duffing oscillator with fractional damping term and multi-frequency force in the form

$$\dot{x} = y, \tag{2a}$$

$$\dot{y} = \omega_0^2 \, x - \beta \, x^3 + \epsilon \left[-\alpha \, \dot{x} \, |\dot{x}|^{P-1} + \sum_{i=1}^{k} f_i \sin \omega_i t \right], \tag{2b}$$

where ϵ is a small parameter.

The fixed points and the phase portrait are derived corresponding to the unperturbed system. If, we let $\epsilon = 0$, the unperturbed system can be written as:

$$\dot{x} = y, \qquad \dot{y} = \alpha^2 x - \beta x^3,$$

which corresponds to an integrable Hamiltonian system with the potential function given by

$$V(x) = -\frac{1}{2}\alpha^2 x^2 + \frac{1}{4}\beta x^4.$$

Shape of the potential function is shown in Figure 1(a) and whose associated Hamiltonian function is

$$H(x, y) = \frac{1}{2} \, y^2 - \frac{1}{2}\alpha^2 \, x^2 + \frac{1}{4}\beta \, x^4.$$

By analyzing the unperturbed ($\epsilon = 0$) part, the system (2) has one saddle point $(x^*, y^*) = (0, 0)$ and the center type fixed point $(x^*, y^*) = (\pm\sqrt{\omega_0^2/\beta}, 0)$. The saddle point is connected to itself by two homoclinic orbits. The two homoclinic orbits $(W^{\pm}(x_h(\tau), y_h(\tau)))$ connecting the saddle to itself
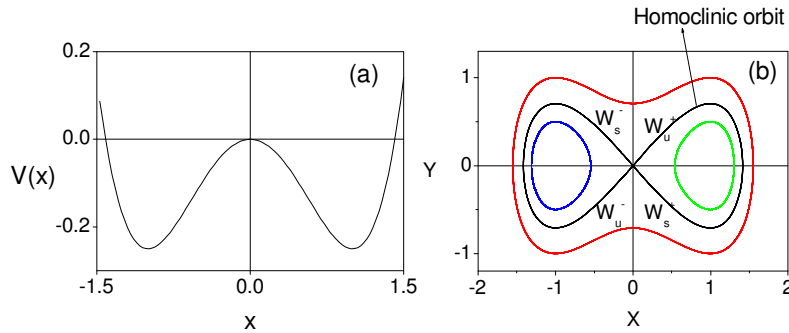
Figure 1: (a) The two-well potential function for the unperturbed system (2). (b) Phase trajectories of the unperturbed system (2). The stable $(W_s^{\pm})$ and unstable $(W_u^{\pm})$ parts of homoclinic orbits, connecting saddle to itself, are indicated. The analytical expression for the homoclinic orbits is given by Eqs. (3).

are given by

$$x_h(\tau) = \pm\sqrt{\frac{2\omega_0^2}{\beta}}, \tag{3a}$$

$$y_h(\tau) = \mp\omega_0^2 \; \sqrt{2/\beta} \; \operatorname{sech}\left(\sqrt{\omega_0^2}\tau\right) \; \tanh\left(\sqrt{\omega_0^2}\tau\right), \quad \tau = t - t_0. \tag{3b}$$

For $\epsilon = 0$, the stable and unstable branches of homoclinic orbits join smoothly. When the dissipative perturbation is included, the stable manifolds $(W_s^{\pm})$ and unstable manifolds $(W_u^{\pm})$ do not join. However, above certain critical amplitude of the external periodic force, transverse intersections of $W_s^{\pm}$ and $W_u^{\pm}$ occur. The presence of such intersections implied the Poincaré map has the so called *horseshoe chaos* [6, 27]. This can be conveniently obtained by the Melnikov function which measures the distance between stable and unstable manifolds. Stable manifolds $(W_s^{\pm})$ and unstable manifolds $(W_u^{\pm})$ of homoclinic orbits are indicated in Figure 1(b). Periodic orbits are nested within and outside the homoclinic orbits.

The Melnikov function for the system (2) along the homoclinic orbits (Eq. (3)) could be computed as follows:

$$M(t_0) = -\alpha \int_{-\infty}^{+\infty} |y_h|^{P+1}d\tau + \int_{-\infty}^{+\infty} y_h \sum_{i=1}^{k} f_i \sin\omega_i \left(\tau + t_0\right) d\tau$$

$$= \qquad I_1 \qquad + \qquad I_2. \tag{4}$$

By the application of some algebraic techniques the integrals I_1 and I_2 can be calculated as follows. The evaluation of the integrals I_1 and I_2 give the following results.

$$I_1 = -\alpha \int_{-\infty}^{\infty} \mid y_h \mid^{P+1} d\tau$$

$$= -\alpha(\omega_0^2)^{P+\frac{1}{2}} \left(\frac{2}{\beta}\right)^{\frac{P+1}{2}} \text{ß} \left[\frac{P+2}{2}, \frac{P+1}{2}\right].$$

Similarly, the integral I_2 is worked out to be

$$I_2 = \int_{-\infty}^{+\infty} y_h \sum_{i=1}^{k} f_i \sin \omega_i (\tau + t_0) d\tau$$

$$= \sum_{i=1}^{k} f_i \cos \omega_i t_0 \int_{-\infty}^{\infty} y_h \sin \omega_i \tau d\tau + \sum_{i=1}^{k} f_i \sin \omega_i t_0 \int_{-\infty}^{\infty} y_h \cos \omega_i \tau d\tau$$

$$= \qquad I_{21} \qquad + \qquad I_{22}.$$

Since $I_{22} = 0$, thus, the value of integral I_{21} is worked out to be

$$I_2 = \mp \pi \sqrt{2/\beta} \sum_{i=1}^{k} f_i \omega_i \text{ sech} \left[\frac{\pi \omega_i}{2\sqrt{\omega_0^2}}\right] \cos \omega_i t_0. \tag{5}$$

Then, the Melnikov function for the Duffing system subjected to fractional damping and multi-frequency excitation term is

$$M^{\pm}(t_0) = -\alpha(\omega_0^2)^{P+\frac{1}{2}} \left[\frac{2}{\beta}\right]^{\frac{P+1}{2}} \text{ß} \left[\frac{P+2}{2}, \frac{P+1}{2}\right]$$

$$\mp \pi \sqrt{2/\beta} \sum_{i=1}^{k} f_i \omega_i \text{ sech} \left[\frac{\pi \omega_i}{2\sqrt{\omega_0^2}}\right] \cos \omega_i t_0.$$

That is,

$$M^{\pm}(t_0) = A \mp B \sum_{i=1}^{k} f_i \omega_i \text{ sech} \left[\frac{\pi \omega_i}{2\sqrt{\omega_0^2}}\right] \cos \omega_i t_0, \tag{6a}$$

where,

$$A = -\alpha(\omega_0^2)^{P+\frac{1}{2}} \left[\frac{2}{\beta}\right]^{\frac{P+1}{2}} \text{ß} \left[\frac{P+2}{2}, \frac{P+1}{2}\right], \tag{6b}$$

$$B = \pi \sqrt{\frac{2}{\beta}}. \tag{6c}$$

where ß(m, n) is the Euler Beta function dependent on arbitrary complex arguments with real parts $[\mathrm{Re}[m] > 0$ and $\mathrm{Re}[n] > 0]$ which is defined as

$$\text{ß}(m, n) = \frac{\Gamma(m)\Gamma(n)}{\Gamma(m + n)},$$

where, $\Gamma(n)$ denotes the Euler Gamma function

$$\Gamma(n) = \int_0^\infty e^{-x}\, x^{n-1}\, dx, \quad \text{where} \quad n > 0$$

3   Horseshoe chaos

In the section, the occurrence of horseshoe chaos in the system (2) driven by multi-frequency force with fractional damping is analyzed. For $k = 1$, we can write the threshold condition on the parameter f for the occurrence of horseshoe chaos. For arbitrary values of ω_i, $i = 1, 2, \ldots, k$ and for $k > 1$ threshold condition on f similar to the case $k = 1$ cannot be written for the onset of horseshoe chaos. However, we can study the occurrence of the horseshoe chaos numerically by measuring the time τ_M elapsed between the two successive changes in the sign of $M(t_0)$. τ_M can be determined from Eq. (6). we fix the parameters in Eq. (2) as $\alpha = 0.5, \beta = 1.0, \omega_0^2 = 1.0$ and $\omega_i = i\omega_1$ with $\omega_1 = 1.0$.

   Figure 2 shows the variation of $1/\tau_M^{\pm}$ versus f for $k = 1$ and some values of P. Continuous curve represents the inverse of first intersection time $(1/\tau_M^+)$ of stable and unstable branches of homoclinic orbits W^+. Dashed curve corresponds to the orbits of W^-. Horseshoe dynamics does not occur when $1/\tau$ is zero and it occurs in the region when $1/\tau > 0$. In Figure 2(a), for $P = 0.1$ and $k = 1$, both $(1/\tau_M^+)$ and $(1/\tau_M^-)$ are zero in the interval $0 < f < 0.7325$. This implies that horseshoe chaos does not occur for $f < f_M^{\pm} = 0.7325$. For $f > f_M^{\pm} = 0.7325$, both $M^+(t_0)$ and $M^-(t_0)$ oscillate and hence $1/\tau_M^{\pm}$ are nonzero. This implies that horseshoe chaos is possible in this region. The variation of $1/\tau_M^{\pm}$ versus f for $P = 0.5, 1.0, 2.0$ are shown in Figure 2(b), Figure 2(c) and Figure 2(d). The Melnikov threshold values for $P = 0.5, 1.0, 2.0$ are $f_M^{\pm} = 0.524, 0.3685$ and 0.2095, respectively. The Figure 2 indicates that the Melnikov threshold for horseshoe (f_M) decreases when P increases. The above analytical results are verified numerically. The Figure 3 shows the variation of $1/\tau_M^{\pm}$ versus f for $k = 3$ and few values of P. For $k = 3$ and $P = 0.1$, $(1/\tau_M^+)$ and $(1/\tau_M^-)$ are zero for $f < f_M^+ = 1.0402$ and $f < f_M^- = 0.4632$ respectively. Horseshoe chaos does not occur for $f < f_M^- = 0.4632$. For f values in the interval $f_M^- < f < f_M^+$, $M^-(t_0)$ alone oscillate which implies that the horseshoe chaos can take
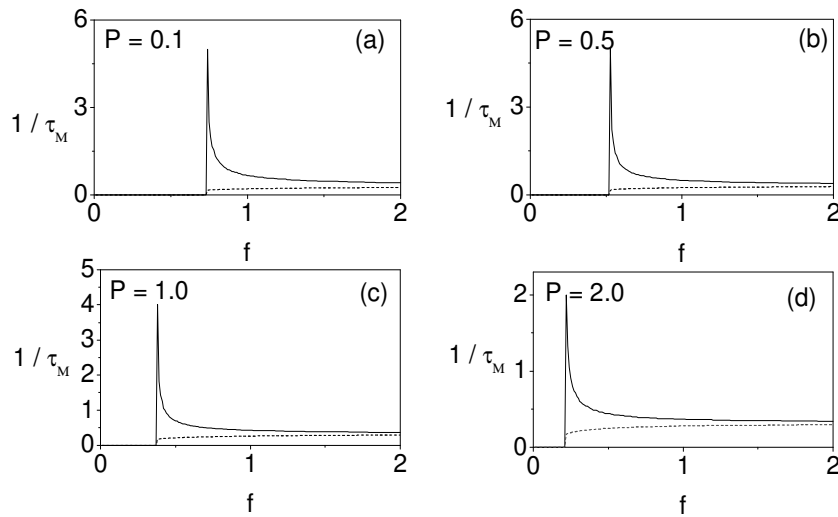
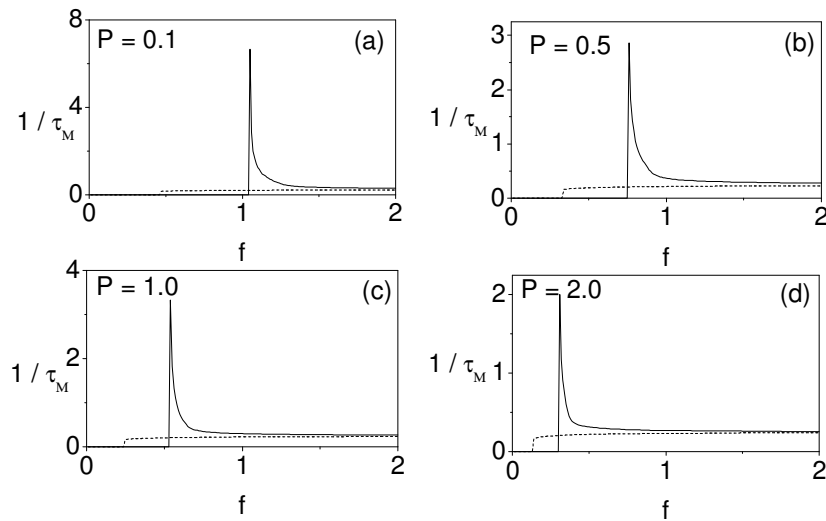Figure 2: Variation of $1/\tau_M$ versus f for $k = 1$ and four values of P.

Figure 3: Variation of $1/\tau_M$ versus f for $k = 3$ and four values of P.

place only in the region $x < 0$. For $f \geq f_M^+$ horseshoe chaos can occur in both the regions $x < 0$ and $x > 0$. The Melnikov threshold values for
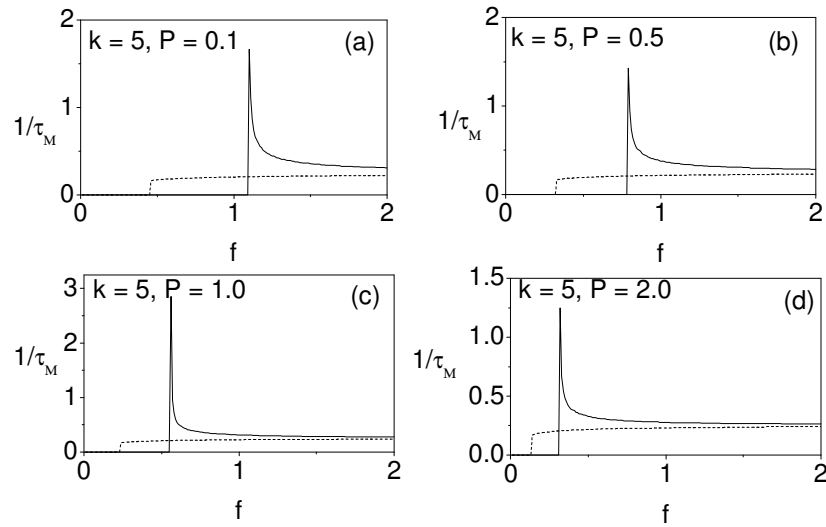
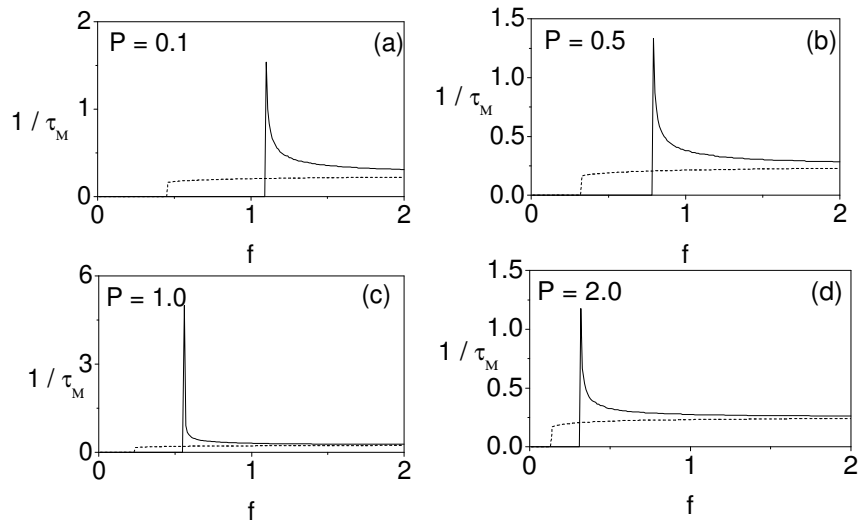Figure 4: Variation of $1/\tau_M$ versus f for $k = 5$ and four values of P.

Figure 5: Variation of $1/\tau_M$ versus f for $k = 10$ and four values of P.

$P = 0.5$, we find $f_M^+ = 0.75$ and $f_M^- = 0.33$; for $P = 1.0$, $f_M^+ = 0.53$ and $f_M^- = 0.24$ and for $P = 2.0$, $f_M^+ = 0.32$ and $f_M^- = 0.13$. The results are also verified numerically.

The variation of $1/\tau_M^\pm$ versus amplitude of the force f for $k = 5$ and $k = 10$ with $P = 0.1, 0.5, 1.0, 2.0$ are shown in the Figure 4 and Figure 5. For $k = 5$ and $k = 10$ the Melnikov threshold values $(f_M^\pm)$ are almost the same. That is, for $k \geq 5$, the variation of $(f_M^\pm)$ is negligible. So inclusion of higher-order frequencies does not have a strong influence on the threshold values of horseshoe chaos, which is clearly evident in the Figure 4 and Figure 5. In the Figure 4 and Figure 5, the Melnikov threshold values for $P = 0.5$, $k = 5$ and $k = 10$, we find $f_M^+ = 1.09$, $f_M^- = 0.45$; for $P = 1.0$, $f_M^+ = 0.55$, $f_M^- = 0.23$ and $P = 2.0$, $f_M^+ = 0.32$, $f_M^- = 0.13$. Here again the values of onset of horseshoe chaos decrease when the damping exponent (P) increases from small values.

4   Numerical Simulations

In this section, we verify the analytical prediction by direct numerical simulation of the system (1). As an example, Figure 6 shows the numerically computed W^s and W^u of the saddle in the Poincaré map for $P = 0.5$ and $P = 2.0$ with $k = 3$. The unstable manifolds are obtained by integrating the Eq. (1) in the forward time for a set of 200 initial conditions chosen around the perturbed saddle point. The stable manifolds are obtained by integrating the equation of motion in reverse time. For clarity only part of the manifolds are shown. Left side of the Figures 6(a-c) show the part of stable and unstable orbits in the Poincaré map for three values of f chosen in Figure 3(b) with $P = 0.5$ and $k = 3$. Transverse intersections of stable and unstable branches of both the homoclinic orbits are seen in Figure 6(c) for $f = 1.0$ (which is above the threshold value $f_M^+ = 0.75$). For $f = 0.5$ (which is in between f_M^- and f_M^+) we see the transverse intersections of W_s^- and W_s^+ orbits alone at two places, which is clearly evident in Figure 6(b). The stable and unstable orbits are well separated in Figure 6(a) for $f = 0.2$ (which is below f_M^-). Horseshoe chaos does not occurs in this region. Right side of the Figures 6(d-f) show the part of stable and unstable orbits in the Poincaré map for three values of f chosen in the Figure 3(d) with $k = 3$ and $P = 2.0$. Transverse intersections of stable and unstable branches of both the homoclinic orbits are seen in Figure 6(d) for $f = 0.5$ (which is above the threshold value $f_M^+ = 0.32$). For $f = 0.2$ (which is in between f_M^- and f_M^+) we see the transverse intersections of W_u^- and W_u^+ orbits alone at two places, which is clearly evident in Figure 6(e). The stable and unstable
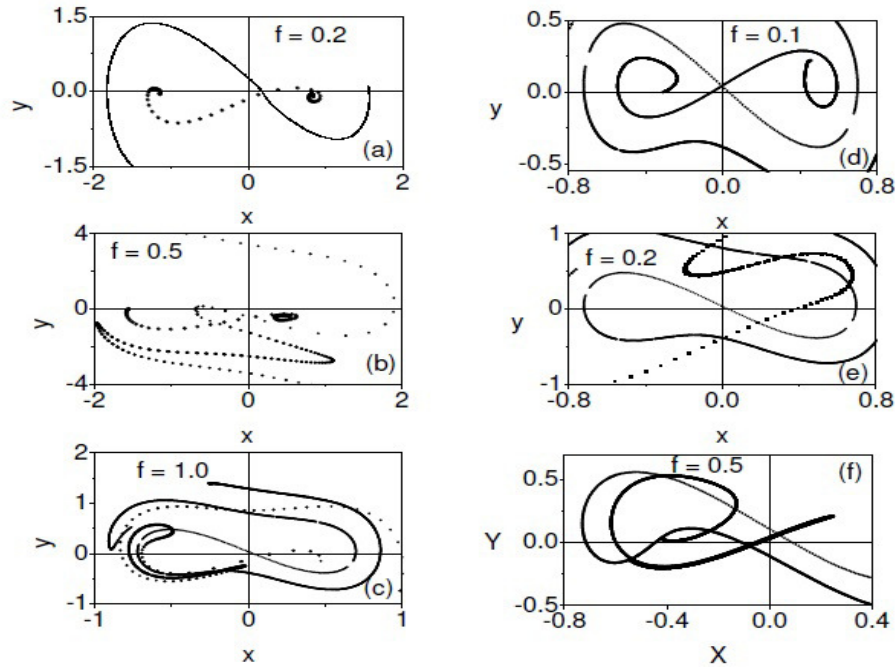
Figure 6: Stable and unstable manifolds of the saddle of the system (2) for three values of f chosen in the Figure 3(b) and Figure 3(c). Left side of the figures for $k = 3$ and $P = 0.5$. Right side of the figures for $k = 3$ and $P = 2.0$.

orbits are well separated in Figure 6(f) for $f = 0.1$ (which is below f_M^-). Horseshoe chaos does not occurs in this region.

In order to know the nature of attractors of the system near the horse-shoe threshold curve, we have further numerically studied the Eq. (2) using Runge-kutta IV order method. We fix the values of parameters as $\alpha = 0.5, \beta = 5.0, P = 2.0, \omega_0^2 = 1.0$ and few values of k. Figure 7(a) shows the bifurcation diagram for $k = 1$. As f is increased from zero, a stable period-T orbit occurs which persists upto $f_c = 0.2512$ and then it loses its stability giving birth to a chaotic orbit. When the parameter f is further increases from f_c one finds that the chaotic orbits persist for a range of f values interspersed periodic windows, period-doubling windows, and intermittency route to chaos. At $f = 0.98521$, chaotic motion suddenly disappears and the long time motion settles to a periodic motion. Similar dynamics is also observed for $k = 3$ in Figure 7(b). The bifurcation pattern for $P = 1.0$ with some values of k is shown in Figure 8. The bifurcation patterns for $k \geq 5$ are almost identical. This is evident from the Figures 7(c-d) and Figures 8(c-d).
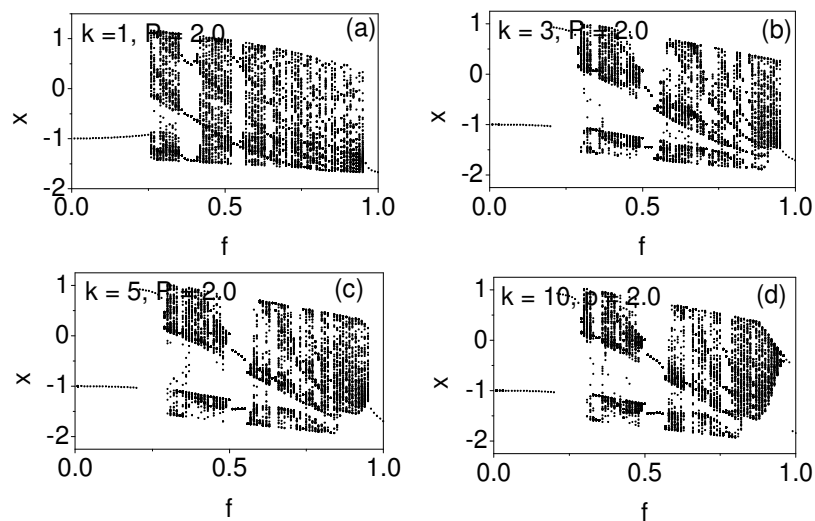
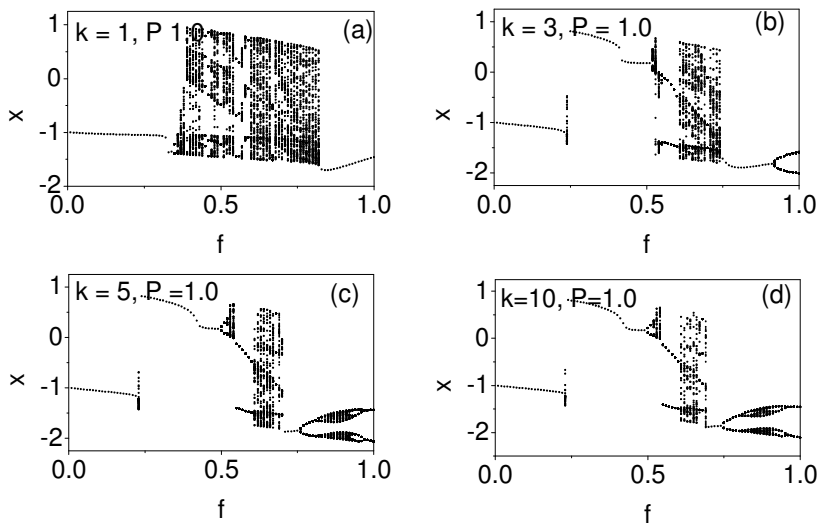Figure 7: Bifurcation diagrams for the system (1) for some values of k with $P = 2.0$.

Figure 8: Bifurcation diagrams for the system (1) for some values of k with $P = 1.0$.

5   Conclusion

In the present paper, we have performed a numerical and analytical predictions of horseshoe chaos in duffing oscillator with fractional damping term and multi-frequency force. For multi-frequency excitation, we obtained the Melnikov threshold condition for onset of horseshoe chaos as $f_m^- = f_m^+$ for $k = 1$. That is onset of horseshoe chaos is obtained at the same value of f in the left- and right-wells. But, for $k > 1$ (that is higher order frequencies), we have $f_m^- \neq f_m^+$, when $f_m^- < f_m^+$ the horseshoe chaos occurs only in the region $x < 0$ for $f \in [f_m^-, f_m^+]$ and $f_m^- > f_m^+$ horseshoe chaos occurs in the $x > 0$ region. We demonstrated the effect of fractional damping on the dynamics of the system. When the damping exponent increases, the threshold for onset of horseshoe chaos decreases. The influence of the higher-order frequencies ($k \geq 5$) does not have a strong influence on the onset of horseshoe chaos, that is, the dynamics of the system is almost the same. We verified the analytical prediction through numerical simulation. It is important to analyze the fractional damping and multi-frequency excitation on certain nonlinear resonance like stochastic and vibrational resonances. These will be investigated in the future.

Acknowledgements

References

[1] J.P. Baltanas, J.L. Trueba and M.A.F. Sanjuan, *Energy dissipation in a nonlinearly damped Duffing oscillators*, Physica D **159** (2001) 22-34.

[2] M. Borowice, G. Litak and A. Syta, *Vibration of the Duffing oscillator; effect of fractional damping*, Shock Vib. **14** (2007) 29-36.

[3] R. Chacon, *Control of homoclinic chaos by weak periodic perturbations*, Singapore, World Scientific, 2005.

[4] A.M. Elnagar and A.F. El-Bassiouny, *Response of self-excited three-degree of freedom systems to multifrequency excitations*, Int. J. Theor. Phys. **31** (1992) 1531-1548.

[5] A.F. El-Bassiouny and G.M. Abed El-Latif, *Resonances in nonlinear structure vibrations under multifrequency excitations*, Phys. Scr. **74** (2006) 410-421.

[6] J. Guckenheimar and P. Holmes, *The nonlinear oscillations, dynamical systems and bifurcations of vector fields*, Springer, New York, 1983.

[7] A. Ibrahim, N. Jaber, A. Chandran and M. Thirupathi, *Dyanmics of microbeams under multi-frequency excitations*, Micromachines **8** (2017) 32-46.

[8] S. Ilyas, A. Ramani, A. Arevalo and M.I. Younis, *An experimental and theoretical invetigation of a micromirror under mixed-frequency excitation*, J. Microelectromech. Syst. **24** (2015) 1124-1131.

[9] N. Jaber, A. Ramani and M.I. Younis, *Multifrequency excitation of a clamped-clamped microbeam: analytical and experimentsl investigation*, Microsyst. Nanoeng **2** (2016) 16002. 10.1038/micronano.2016.2.

[10] N. Jaber, A. Ramani, Q. Hennawi and M.I. Younis, *Wideband MEMS resonator using multifrequency excitation*, Sens. Actuators A Phys. **242** (2016) 140-145.

[11] A.J. Lichtenberg and M.A. Lieberman, *Regular and stochastic motion*, Springer-Verlag, New York, 1990.

[12] R. Lima and M. Pettini, *Parametric resonant control of chaos*, Int. J. Bifur. Chaos Appl. Sci. Eng. **8** (1998) 1675-1684.

[13] V.K. Melnikov, *On the stability of the center for time periodic perturbations*, Trans. Moscow Math. Soc. **12** (1963) 1-56.

[14] Yu.I. Neimark and P.S. Landa, *Stochastic and chaotic oscillations*, Kluwer Academic, Dordrecht, 1987.

[15] A. Ramani, A.I. Ibrahim and M.I. Younis, *Mixed frequency excitation of an electrostatically actuated resonator*, Moicrosyst. Technol. **22** (2016) 1967-1974

[16] V. Ravichandran, V. Chinnathambi and S. Rajasekar, *Horseshoe dynamics in Duffing oscillator with multifrequency excitation*,Nonlinear Dynamics, Editors: M. Daniel and S. Rajasekar, Narosa Publishing House, New Delhi, India, 2009.

[17] V. Ravichandran, V. Chinnathambi and S. Rajasekar, *Effect of rectified and modulated sine forces on chaos in Duffing oscillator*, Indian J. Phys. **83(1)** (2009) 1593-1603.

[18] V. Ravichandran, V. Chinnathambi and S. Rajasekar, *Homoclinic bifurcations and chaos in Duffing oscillator driven by an amplitude modulated force*, Physica A **37** (2007) 223-236.

[19] V. Ravichandran, S. Jeyakumari, V, Chinnathambi S. Rajaseakr and M.A.F. Sanjuan, *Role of asymmetries in the chaotic dynamics of the double-well Duffing oscillator*, Pramana J. Phys. **72(6)** (2009) 927-937.

[20] L. Ravisankar, V. Ravichandran and V. Chinnathambi, *Predictions of Horseshoe chaos in DVP oscillator driven by different periodic forces*, Int. J. Engg. Sci. **1(5)** (2012) 17-25

[21] L. Ravisankar, V. Ravichandran, V. Chinnathambi and S. Rajasekar, *Horseshoe dynamics in asymmetric Duffing-vander pol oscillator driven by narrow band frequency modulated force*, Chinese J. Phys. **52(3)** (2014) 1026-1043.

[22] M.A.F. Sanjuan, *The effect of nonlinear damping on the universal escape oscillator*, Int. J. Bifur. and Chaos **9** (1999) 735-744.

[23] M.V. Sethu Meenakshi, S. Athisayanathan, V. Chinnathambi, S. Rajasekar, *Analytical estimates of the effect of amplitude modulated signal in nonlinearly damped Duffing-vander Pol oscillator*, Chinese J. Phys. **55** (2017) 2208-2217.

[24] M.V. SethuMeenakshi, S. Athisayanathan, V. Chinnathambi, S. Rajasekar, *Effect of narrow band frequency modulated signal on Horseshoe chaos in nonlinearly damped Duffing-vander Pol oscillator*, Annu. Rev. Chaos Theory Bifurcations Dyn. Syst. **7** (2017) 41-55.

[25] M. Siewe Siewe, F.M. Moukam Kakmeni and C. Tchawona, *Resonant oscillation and homoclinic bifurcation in a ϕ^6-Vander Pol oscillator*, Chaos Solitons Fractals **21** (2004) 841-853.

[26] J.L. Trueba, J. Rams and M.A.F Sanjuan, *Analytical estimates of the effect of nonlinear damping in some nonlinear oscillators*, Int. J. Bifur. and Chaos **109** (2000) 2257-2267.

[27] S. Wiggins, *Introduction to applied nonlinear dynamical systems and chaos*, Springer, New York, 1990.